Synthesis and Characterization of Large Colloidal Silver Particles

Krassimir P. Velikov,*,†,§ Gabby E. Zegers,† and Alfons van Blaaderen*,†,‡

Soft Condensed Matter, Debye Institute, Utrecht University, Princetonlaan 5, 3584 CC Utrecht, The Netherlands, and FOM Institute for Atomic and Molecular Physics, Kruislaan 407, 1098 SJ Amsterdam, The Netherlands

Received September 26, 2002. In Final Form: November 22, 2002

Metal colloidal particles are widely used as building blocks for novel materials with photonic applications. In this article, we demonstrate the synthesis of silver particles with a wide range of sizes (up to 1200 nm in radius) by reducing silver nitrate with ascorbic acid in aqueous solutions in the presence of a polymeric steric stabilizer. The resulting particles were spherical aggregates with a rough surface and polydispersity below 20%. The particle morphology was examined by electron microscopy. Silver particles were directly coated with silica in a seeded growth Stöber process. Optical properties on a single-particle level were studied by means of extinction measurements and compared to scattering theory. At low ionic strength, the effective polydispersity of the charged silver particles was low enough to form a colloidal crystal.

Introduction

Colloidal metal and metallodielectric particles are of great fundamental and industrial interest. Metal colloidal particles are used in catalysis,[1,2] biological and chemical sensing,[3] nonlinear optics,[4−6] surface-enhanced Raman spectroscopy (SERS),[7,8] and electronics.[9] Recently, metal and metallodielectric spheres found new applications in the field of photonic crystals.[10−14] Photonic crystals are materials with a periodically modulated dielectric constant.[15−17] In analogy to electrons in semiconductors, electromagnetic wave propagation in photonic crystals can be forbidden for a certain frequency range resulting in the formation of a complete photonic band gap (CPBG); photons in the gap cannot travel in any direction for any polarization. It has been shown theoretically that in a face-centered-cubic (fcc) crystal of metal or metallodielectric spheres a CPBG in the visible or near-IR can be opened.[10−12] Because of the high dielectric contrast necessary (>2.8 for air-sphere fcc crystals[18,19]), it is difficult to create a CPBG with purely dielectric materials. To build photonic crystals, the size of the particles should be comparable to the wavelength of light. The second important requirement is to use particles with low absorption in the region of application. A few metals (Ag, Au, Al, Ni, Cu) have been investigated theoretically as possible candidates for metallodielectric photonic crystals.[10−14] Because of its low bulk absorption, silver (Ag) is the most suitable metal to create a CPBG in the visible. Recent calculations of Moroz have shown that a CPBG can even be opened up for a filling fraction of silver as low as 2%.[20]

Several methods have been developed to synthesize colloidal metal particles.[21−23] These are precipitation from homogeneous solutions by using appropriate reducing agents,[24,25] seeded growth,[26] reverse micelles,[27,28] and electrochemical[29] and sonoelectrochemical[30] techniques. Among these, precipitation in aqueous or nonaqueous media is the most commonly used because it is easy, cheap, and versatile. The precipitation technique offers many possibilities to control the particle characteristics by changing the experimental parameters, such as reactant concentrations, temperature, pH, reducing agents, and stabilizators.[21,31,32] Furthermore, it is also possible to

* To whom correspondence should be addressed. E-mail: A.vanBlaaderen@phys.uu.nl, Krassimir.Velikov@Unilever.com.
† Utrecht University.
‡ FOM Institute for Atomic and Molecular Physics.
§ Present address: Unilever Research, Olivier van Noortlaan 120, P.O. Box 114, 3130 AC Vlaardingen, The Netherlands.

(1) Gates, B. C.; Guezi, L.; Knosinger, H. *Metal clusters in catalysis*; Elsevier: Amsterdam, 1986.
(2) Jana, N. R.; Sau, T. K.; Pal, T. *J. Phys. Chem. B* **1999**, *103*, 115.
(3) Elghanian, R.; Storhoff, J. J.; Mucic, R. C.; Letsinger, R. L.; Mirkin, C. A. *Science* **1997**, *277*, 1078.
(4) Olsen, A. W.; Kafafi, Z. H. *J. Am. Chem. Soc.* **1991**, *113*, 7758.
(5) Ganeev, R. A.; Ryasnyanskii, A. I.; Kodirov, M. K.; Kamalov, S. R.; Usmanov, T. *Opt. Spectrosc.* **2001**, *90*, 568.
(6) Ganeev, R. A.; Ryasnyansky, A. I.; Kamalov, S. R.; Kodirov, M. K.; Usmanov, T. *J. Phys. D: Appl. Phys.* **2001**, *34*, 1602.
(7) Kambhampati, D. K.; Knoll, W. *Curr. Opin. Colloid Interface Sci.* **1999**, *4*, 273.
(8) Nie, S. M.; Emery, S. R. *Science* **1997**, *275*, 1102.
(9) Tominaga, J.; Mihalcea, C.; Buchel, D.; Fukuda, H.; Nakano, T.; Atoda, N.; Fuji, H.; Kikukawa, T. *Appl. Phys. Lett.* **2001**, *78*, 2417.
(10) Moroz, A. *Phys. Rev. Lett.* **1999**, *83*, 5274.
(11) Moroz, A. *Europhys. Lett.* **2000**, *50*, 466.
(12) Zhang, W. Y.; Lei, X. Y.; Wang, Z. L.; Zheng, D. G.; Tam, W. Y.; Chan, C. T.; Sheng, P. *Phys. Rev. Lett.* **2000**, *84*, 2853.
(13) El-Kady, I.; Sigalas, M. M.; Biswas, R.; Ho, K. M.; Soukoulis, C. M. *Phys. Rev. B* **2000**, *62*, 15299.
(14) Wang, Z.; Chan, C. T.; Zhang, W.; Ming, N.; Sheng, P. *Phys. Rev. B* **2001**, 113108.
(15) Yablonovitch, E. *Phys. Rev. Lett.* **1987**, *58*, 2059.
(16) John, S. *Phys. Rev. Lett.* **1987**, *58*, 2486.
(17) Bykov, V. P. *Sov. J. Quantum Electron.* **1975**, *4*, 861.
(18) Biswas, R.; Sigalas, M. M.; Subramania, G.; Ho, K. M. *Phys. Rev. B: Condens. Matter* **1998**, *57*, 3701.
(19) Busch, K.; John, S. *Phys. Rev. E* **1998**, *58*, 3896.
(20) Moroz, A. *Phys. Rev. B* **2002**, *66*, 115109.
(21) Goia, D. V.; Matijevic, E. *New J. Chem.* **1998**, *22*, 1203.
(22) Adair, J. H.; Li, T.; Kido, T.; Havey, K.; Moon, J.; Mecholsky, J.; Morrone, A.; Talham, D. R.; Ludwig, M. H.; Wang, L. *Mater. Sci. Eng., R* **1998**, *23*, 139.
(23) Adair, J. H.; Suvaci, E. *Curr. Opin. Colloid Interface Sci.* **2000**, *5*, 160.
(24) Mayer, A. B. R.; Hausner, S. H.; Mark, J. E. *Polym. J.* **2000**, *32*, 15.
(25) Chou, K. S.; Ren, C. Y. *Mater. Chem. Phys.* **2000**, *64*, 241.
(26) Hachisu, S. *Croat. Chem. Acta* **1998**, *71*, 975.
(27) Taleb, A.; Petit, C.; Pileni, M. P. *Chem. Mater.* **1997**, *9*, 950.
(28) Egorova, E. M.; Revina, A. A. *Colloids Surf., A* **2000**, *168*, 87.
(29) Rodriguez-Sanchez, L.; Blanco, M. C.; Lopez-Quintela, M. A. *J. Phys. Chem. B* **2000**, *104*, 9683.
(30) Zhu, J. J.; Liu, S. W.; Palchik, O.; Koltypin, Y.; Gedanken, A. *Langmuir* **2000**, *16*, 6396.
(31) Matijevic, E. *Chem. Mater.* **1993**, *5*, 412.
(32) Matijevic, E. *Langmuir* **1994**, *10*, 8.

10.1021/la026610p CCC: $25.00
Published on Web 01/18/2003

synthesize composite particles and alloys.[33−35] Because of the high electropositive character of silver (+0.799 V[36]), various reducing agents[21] including free radicals,[37] sodium borohydrate ($NaBH_4$),[38] citrate or ethylenediaminetetraacetic acid (EDTA),[39] and ethanol[40] can be used. However, most methods known for the preparation of metal spheres were developed to produce small particles (radius less than 100 nm). Only recently, gold particles with a radius up to 2 μm were synthesized by controlled aggregation of gold nanoparticles using gum arabic as a steric stabilizer.[21] Coating of colloidal particles with a silica layer has many advantages, because it allows for surface modification, decreases the polydispersity of the particles, and reduces the van der Waals attraction leading to enhanced colloidal stability. Coating with silica has been demonstrated for many metal particles.[41−47] Direct coating with silica was only recently reported for surfactant-stabilized silver particles.[48]

In this article, we will describe the synthesis of silver particles of a wide range of sizes and narrow size distribution by reducing silver nitrate with ascorbic acid in an aqueous medium. The particle morphology was studied by electron microscopy. Optical response on a single-particle level was studied by means of extinction measurements and compared to scattering theory. The formation of charge-stabilized colloidal crystals and colloidal glasses of the silver particles in water was studied by reflection confocal microscopy.

Experimental Section

Materials. All reagents and solvents were used as received without further purification. Ultrapure grade silver nitrate ($AgNO_3$) was purchased from Acros Organics, gum arabic from Sigma, ascorbic acid ($C_6O_8H_6$) from PG Farma, sodium hydroxide (NaOH) from Baker Chemicals B.V., ammonia (29.3 wt % NH_3) of analytical reagent quality from Merck, and tetraethoxysilane (TES) of puriss. grade quality from Fluka. Absolute technical grade ethanol (NEDALCO) or analytical grade ethanol (Merck) and Milli-Q water were used in all preparations.

Particle Synthesis. A variable amount of a silver nitrate stock solution was added to a variable amount of a stock solution of gum arabic and filled up to a controlled volume with deionized water. In the same way, a solution containing controlled amounts of ascorbic acid and gum arabic was prepared and then filled up to a certain volume. The pH of the reaction mixture was set at this stage by adding a controlled volume of NaOH to the ascorbic acid solution. Both reactant solutions always contained the same weight percentage of gum arabic. The reactions were carried out in a two-necked round-bottom flask of 250 mL with a magnetic stirrer or with a variable high-speed electric stirrer (1100 rpm). First, the solution containing the ascorbic acid was put into the reaction flask. Then, the silver solution was quickly added to the vigorously stirred acid solution. As a result of the size-dependent extinction of the silver particles, the color of the solution turned from transparent to black and then to dark brown-grayish as the scattering contribution increased. After several hours (∼2−4 h), the solution became brownish to green-brownish. The induction time (a few seconds) for these colors to appear was dependent on the reaction conditions. The solutions were stirred up to 24 h at room temperature. Subsequently, the dispersions were washed twice with deionized water after sedimentation or centrifugation (max 200*g*). The silver particles were kept in water where they remained stable longer than a year.

Coating with Silica. A silica shell around silver particles was formed without using a silane coupling agent. An ammonia solution (1.0 g of ammonia (29.3 wt % NH_3) in 25 mL of ethanol) was added to a 10 mL suspension ($\sim 10^{-2}$ vol %) of silver particles ($R = 320$ nm) in ethanol under magnetic stirring. Subsequently, 87.2 μL of TES solution (10.0 vol % in ethanol) was added. The reaction mixture was stirred for 24 h. The resulting particles were separated by centrifugation and redispersed in pure ethanol.

Particle Characterization. The particle morphology was studied by transmission electron microscopy (TEM) and scanning electron microscopy (SEM) on a Philips CM10 and on a Philips XL30 FEG, respectively. The particle size and polydispersity were determined from the TEM micrographs using a Nikon profile projector. Thermogravimetric analysis (TGA) was performed on a Setaram 92. A Coulter Delsa 440 SX was used to measure the particle electrophoretic mobility in aqueous suspension. UV−vis spectroscopy (Cary 1E UV−vis spectrophotometer) was performed on dilute ($<10^{-5}$ vol %) suspensions of Ag particles in water. The optical path was 1.00 cm. Fitting of the spectra was performed using a FORTRAN computer algorithm developed by Wiscombe,[49] adapted to take the size polydispersity into account. Colloidal crystallization was studied in both little glass vials (1.7 mL), of which the bottom was replaced by a microscope cover glass (Chance Propper, no. 1) with a thickness of 0.17 mm, and thin (0.20 mm) glass capillaries (VitroCom). Charge-stabilized crystals and glasses in water were observed in reflection mode ($\lambda = 632$ nm) with a confocal microscope (Leica DM IRB, in combination with a Leica TCS NT scanhead) with an oil-immersion lens (Leica, 100×, numerical aperture (NA) 1.4).

Results and Discussion

Particle Synthesis. Silver ions were reduced to metal silver by ascorbic acid ($C_6H_8O_6$), which has a sufficiently lower redox potential,[21,50] according to the following reaction:

$$C_6H_8O_6 + 2Ag^+ \rightarrow 2Ag^0 + C_6H_6O_6 + 2H^+$$

Matijevic et al. proposed a particle growth model for a similar synthesis of gold particles.[51] The nucleation burst takes place when the concentration of metal atoms reaches a critical supersaturation. In the first step, the nuclei formed grow to nanosized primary particles by diffusion capture of the remaining atoms. In the second step, depending on the reaction conditions, the primary particles aggregate, leading to the formation of larger spherical aggregates accompanied with narrowing of the size distribution.[51] The precipitation was carried out at different pH values, different concentrations of the protective colloid, and different concentrations of silver and ascorbic acid (Table 1).

(33) Mulvaney, P.; Giersig, M.; Henglein, A. *J. Phys. Chem.* **1993**, *97*, 7061.
(34) Torigoe, K.; Nakajima, Y.; Esumi, K. *J. Phys. Chem.* **1993**, *97*, 8304.
(35) Link, S.; Wang, Z. L.; El-Sayed, M. A. *J. Phys. Chem. B* **1999**, *103*, 3529.
(36) David, R. L. *Handbook of chemistry and physics*, 76th ed.; CRC Press: Boca Raton, FL, 1995−1996.
(37) Henglein, A.; Giersig, M. *J. Phys. Chem. B* **1999**, *103*, 9533.
(38) Wang, W.; Efrima, S.; Regev, O. *Langmuir* **1998**, *14*, 602.
(39) Bright, R. M.; Musick, M. D.; Natan, M. J. *Langmuir* **1998**, *14*, 5695.
(40) Liz-Marzan, L. M.; LadoTourino, I. *Langmuir* **1996**, *12*, 3585.
(41) Ohmori, M.; Matijevic, E. *J. Colloid Interface Sci.* **1993**, *160*, 288.
(42) Liz-Marzan, L. M.; Philipse, A. P. *J. Colloid Interface Sci.* **1995**, *176*, 459.
(43) Liz-Marzan, L. M.; Giersig, M.; Mulvaney, P. *Langmuir* **1996**, *12*, 4329.
(44) Liz-Marzan, L. M.; Giersig, M.; Mulvaney, P. *Chem. Commun.* **1996**, 731.
(45) Giersig, M.; Ung, T.; Liz-Marzan, L. M.; Mulvaney, P. *Adv. Mater.* **1997**, *9*, 570.
(46) Ung, T.; Liz-Marzan, L. M.; Mulvaney, P. *Langmuir* **1998**, *14*, 3740.
(47) Yang, C. S.; Liu, Q.; Kauzlarich, S. M.; Phillips, B. *Chem. Mater.* **2000**, *12*, 983.
(48) Hardikar, V. V.; Matijevic, E. *J. Colloid Interface Sci.* **2000**, *221*, 133.
(49) The original source can be found at http://climate.gsfc.nasa.gov/~wiscombe/.
(50) Goia, D. V.; Matijevic, E. *Colloids Surf., A* **1999**, *146*, 139.
(51) Privman, V.; Goia, D. V.; Park, J.; Matijevic, E. *J. Colloid Interface Sci.* **1999**, *213*, 36.

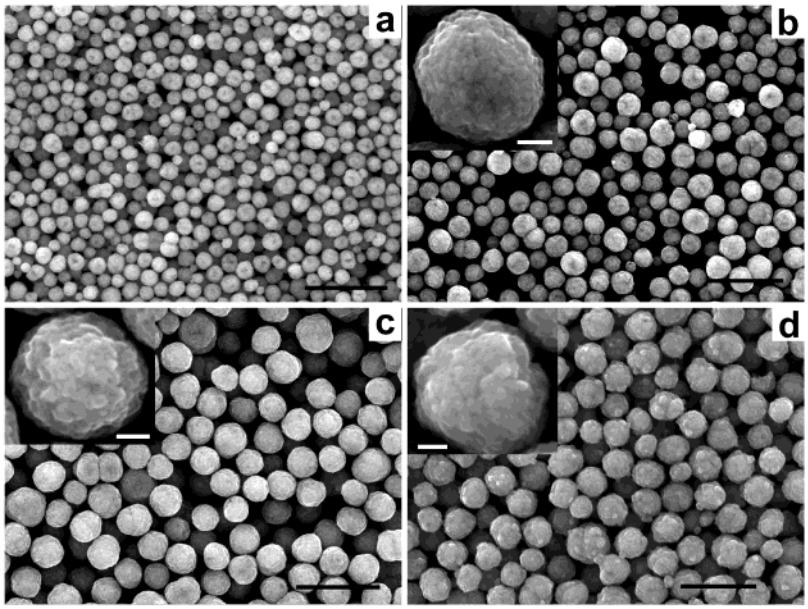

Figure 1. Scanning electron micrographs (SEM) of monodisperse silver particles obtained under different experimental conditions, radii (R), and relative widths of the size distribution (δ): (a) $R = 197$ nm, $\delta = 13\%$; (b) $R = 284$ nm, $\delta = 17\%$; (c) $R = 383$ nm, $\delta = 13\%$; (d) $R = 418$ nm, $\delta = 12\%$. The scale bars are 2 μm. The insets show a blowup of the particle surface. The scale bars in the insets are 200 nm.

Table 1. Radius (R) and Polydispersity (δ) of Silver Particles Obtained at Different Experimental Conditions As Determined by TEM

sample	$[AgNO_3]$ (mol/L)	$[C_6H_8O_6]$ (mol/L)	ratio [acid]/[Ag]	gum arabic wt %	R (nm)	δ (%)
15	0.083	0.333	4	0.7	223	67
11	0.083	0.167	2	0.7	894	24
9	0.083	0.333	4	0.35	429	33
12	0.083	0.167	2	0.35	1149	16
14	0.167	0.666	4	0.7	796	29
16	0.167	0.333	2	0.7	525	39
13	0.167	0.666	4	0.35	943	35
10	0.167	0.333	2	0.35	588	31

The results are strongly dependent on the age of the solutions. Using freshly prepared solutions was necessary to obtain reproducible results. Because of the strong size-dependent extinction, the particle growth can be monitored in the reaction flask through a change in color of the suspension. Because of scattering, the final suspension of large particles had a brownish appearance (see below). Figure 1 shows SEM micrographs of relatively monodisperse silver particles obtained at different experimental conditions. The final particle size depends on the pH of the reaction mixture (Figure 2). At higher pH values, the primary particles have a sufficiently large surface charge, which, possibly in combination with the effect of the protective polymer layer, diminishes the effect of the high ionic strength and prevents significant aggregation. As a result, the final particles are not significantly larger than the primary particles. With a decrease of the pH, the system approaches the isoelectric point and, therefore, becomes less stable leading to a higher degree of aggregation of the primary particles and to the formation of larger secondary particles. This mechanism is quite general and has been proposed for the formation of several inorganic particles.[51,52]

The amount of gum arabic added also influences the aggregation rate. At a higher concentration of gum, the particles became smaller (Table 1). This occurs because

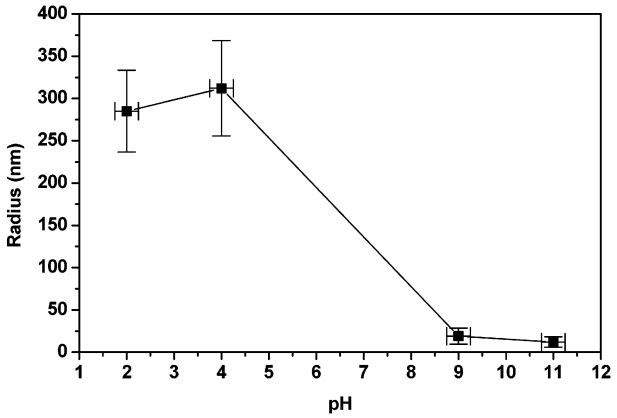

Figure 2. Particle size as a function of the pH of the reaction mixture. The reaction mixture had an initial pH of ~2. The pH was regulated by addition of NaOH solution. Particles were synthesized using the following concentrations: $[AgNO_3] = 0.010$ M; $[C_6O_8H_6] = 0.050$ M; gum arabic, 0.056 wt %.

of the enhanced steric stabilization[53] of the small primary particles, which prevents their aggregation leading to smaller secondary particles. In addition, at high gum concentration the viscosity of the reaction mixture will be increased and the diffusion aggregation of the primary particles will be suppressed. The effect of gum arabic on the reaction was not studied in detail.

As in the case of gold particles,[50] the speed of mixing of the reactants influences the time-dependent supersaturation, that is, the buildup of metal silver in the suspension. When the mixing time is shorter, the silver nucleation takes a shorter amount of time which results in more monodisperse primary particles.[51] If the reactants are added slowly, there will be a continuous generation of nuclei during the mixing. As the first nuclei formed will act like seeds[54] and will further grow to larger sizes before aggregation and forming secondary particles, the primary

(52) Bogush, G. H.; Zukoski, C. F. *J. Colloid Interface Sci.* **1991**, *142*, 19.

(53) Napper, D. H. *Polymeric stabilization of colloidal dispersions*; Academic Press: London, 1983.

(54) Jana, N. R.; Gearheart, L.; Murphy, C. J. *Chem. Mater.* **2001**, *13*, 2313.

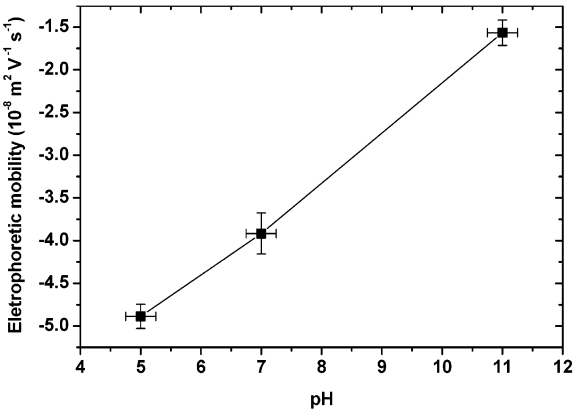

Figure 3. Electrophoretic mobility of silver particles ($R = 256$ nm, $\delta = 17\%$) dispersed in water as a function of the pH.

particles will have a broader size distribution. As a result, the size of the final secondary particles remains approximately the same, but the particle surface is rougher, indicating the presence of larger subunits.

Particle Morphology. By use of the procedure described above, we obtained spherical silver particles with a radius in the range from 100 to 1200 nm. Particle polydispersity was more difficult to control and varied over a wide range. However, a polydispersity as low as 12% was achieved in several samples. The particles are spherical aggregates with a rough surface (see the insets in Figure 1) where the roughness is on the order of a few nanometers. The SEM pictures clearly reveal the aggregated nature of the final particles, which consist of small (<20 nm) subunits. Despite several cleaning cycles, TGA analysis showed that the particles contained ~4% organic compounds, most likely composed of the protective polymer (gum arabic) and perhaps a small amount of ascorbic acid or its derivatives. In addition to the steric stabilization, as a result of the dissociation of the carboxyl groups and the absorption of other different ionic species, the particle surface is charged. Figure 3 shows electrophoretic mobility measurements on silver particles of 256 nm in radius ($\delta = 17\%$) dispersed in water as a function of pH. The particle surface charge is negative over a wide range of pH values including neutral water suspensions. The fact that the electrophoretic mobility decreases at higher pH values indicates some degree of oxidation of the particle surface, which probably occurred after the separation from the reaction mixture. The particle surface charge is determined by the oxide layer and the remaining carboxyl groups attached to the surface. The surface charge plays an important role in the particle self-organization after sedimentation in aqueous suspensions.

Silica-Coated Ag Particles. The presence of an inert dielectric layer around metal particles allows tailoring their properties and interaction potential. For instance, a thin (~20 nm) silica layer is sufficient to screen the van der Waals attraction increasing the particle stability. Silver seeds were directly coated with a silica layer by hydrolysis and condensation of TES in an ethanol−water−ammonia mixture. Figure 4 shows TEM micrographs of Ag particles coated with silica in a one-step seeded growth process. The most important factor during the coating is the stability of the initial seed suspension at the reaction conditions (high pH). Appreciable dissolution of the Ag particles due to the presence of ammonia in the reaction mixture was not observed in the time scale of the coating process. The presence of gum arabic adsorbed on the particle surface facilitates the direct binding of hydrolyzed monomers. If a thin initial layer of silica is already deposited, the coating can be further continued as a simple seeded growth process until the desired thickness is reached.

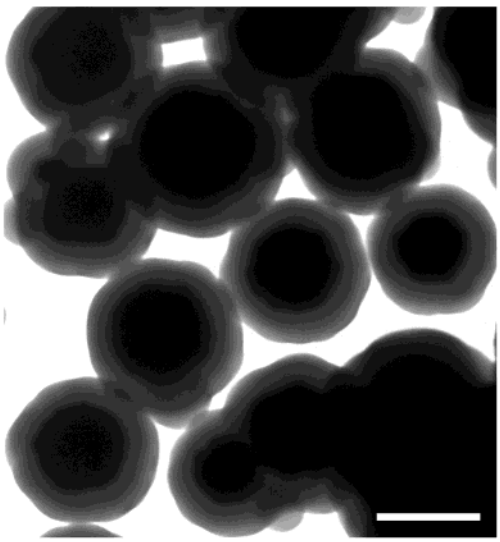

Figure 4. Transmission electron micrographs of silver particles ($R = 300$ nm) coated with silica (~50 nm). The scale bar is 500 nm.

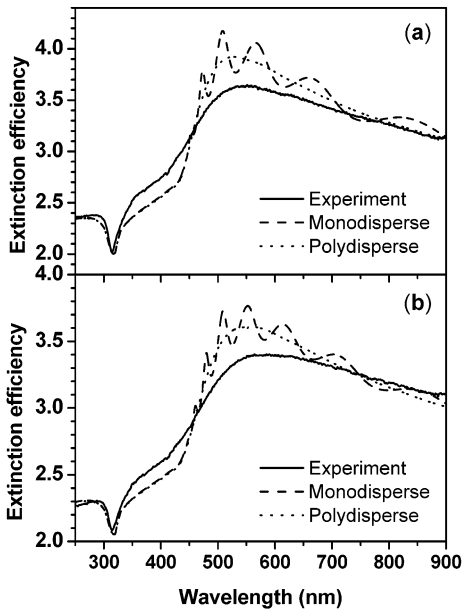

Figure 5. Comparison between the experimental (solid line) and calculated extinction efficiency spectra for monodisperse (dashed line) and polydisperse (dotted line) particles in water. (a) $R = 284$ nm, $\delta = 16\%$ (from TEM); theoretical spectra were calculated using $R = 285$ nm, $\phi_{Ag} = 0.80$. (b) $R = 383$ nm, $\delta = 13\%$ (from TEM); theoretical spectra were calculated using $R = 385$ nm, $\phi_{Ag} = 0.80$. In both cases, the polydispersity was set on 15%.

Optical Properties. When colloidal particles are used for photonic applications (such as in photonic crystals or SERS), it is important to know the optical response on a single-particle level. We performed extinction measurements on dilute suspensions of Ag particles of different radii in water. All spectra were taken in the range of 250−900 nm. Figure 5 shows two examples of experimentally determined extinction efficiency spectra of Ag particles of mean radii 284 and 383 nm. Both spectra display a sharp minimum at ~318 nm, which corresponds to a minimum in the imaginary part of the refractive index (n_{Im} =

$\mathrm{Im}([\epsilon(\lambda)]^{1/2}) \sim 0.4$ for bulk silver[55]). The depth of this minimum depends on the particle radius, but the position, for the sizes studied here, is determined by the dielectric properties of the metal. At longer wavelengths, a broad band due to surface plasma resonances was observed. The position of the peak shifts toward longer wavelengths if the particle size is increased. Our experiments showed that the dependence of the extinction efficiency on the particle radius is not as strong as in the case of dielectric spheres.[56] Because of the complex refractive index of Ag and the size of the particles studied, a full solution of the Maxwell equations is necessary to quantitatively describe the light scattering and absorption by the system. The exact shape of the curves in general is sensitive to particle size, dielectric contrast, and polydispersity. In this case, however, due to the imaginary part of the silver refractive index, fine resonances are damped.[56] The extinction efficiency spectra were calculated using scattering theory extended to the case of polydisperse particles assuming a Gaussian size distribution. The effective dielectric constant of a sphere is represented as an effective dielectric constant of a mixture of a bulk Ag and a dielectric (solvent). The effective dielectric constant, ϵ_{eff}, was calculated using the Bruggeman effective medium model for a randomly connected inhomogeneous medium,[56]

$$\epsilon_{\mathrm{eff}}(\lambda) = \frac{1}{4}[g \pm \sqrt{g^2 + 8\epsilon_{\mathrm{Ag}}(\lambda)\epsilon_{\mathrm{s}}}]$$

where

$$g = (3\phi_{\mathrm{Ag}} - 1)\epsilon_{\mathrm{Ag}}(\lambda) + (2 - 3\phi_{\mathrm{Ag}})\epsilon_{\mathrm{s}}$$

where ϕ_{Ag} is the filling fraction of bulk Ag with a wavelength-dependent dielectric constant $\epsilon_{\mathrm{Ag}}(\lambda)$,[55] and ϵ_{s} is the solvent dielectric constant. The wavelength dependence of the refractive index of the solvent (water $n_{\mathrm{s}} = 1.33$) was neglected. The theoretical spectrum (Figure 5a) was calculated using a particle size and polydispersity determined from TEM and a filling fraction of bulk silver $\phi_{\mathrm{Ag}} = 0.80$. Values in the range of 0.75−0.85 for the filling fraction of silver were found to give the best description of the scattering of all particles studied. Model calculations have shown that the position of the maximum extinction is strongly dependent on the filling fraction of bulk silver (Figure 6a). The theoretical spectra describe the experimental spectra relatively well. However, we could not find a perfect match for the whole extinction curve. Most probably, this is because of the more complicated structure and shape (roughness) of the particles studied and/or the use of an effective medium approximation.

As already mentioned, the absorption of light by metal particles is an important issue. The physical origin of this absorption is the coherent oscillation of the conduction band electrons induced by the electromagnetic field.[57] Scattering theory allows for separation of the scattering and absorption components of the total extinction efficiency (Figure 6b). For large particles, the scattering dominates over the absorption. As a result, for wavelengths longer than 500 nm, the contribution of absorption to the total extinction is less than 5%.

Colloidal Crystallization. Silver particles dispersed in water possess a negative surface charge as inferred from the electrophoretic mobility measurements (Figure 3). The surface charge of the colloidal spheres probably derives from the dissociation of carboxyl groups of the gum arabic and ascorbic acid, which were adsorbed during the synthesis of the spheres, or a thin layer of silver oxide formed thereafter. Figure 7a shows a confocal image in reflection mode of the bottom layer of a charge-stabilized colloidal crystal of Ag spheres of radius 257 nm ($\delta = 17\%$) in water formed at the bottom of a small glass vial. The crystal lattice spacing as determined by reflection confocal microscopy was $\sim 1\,\mu$m, a value which is much larger than the particle diameter. Despite the relatively large size polydispersity of the core, the particles formed single colloidal crystals, which in some cases were hundreds of micrometers in size. It is known from computer simulations and experiments that colloids interacting with a hard-sphere-like potential cannot form colloidal crystals with a polydispersity above ~7%.[58,59] The cores of the silver particles are significantly more polydisperse. The fact that these particles can form crystals, with low filling fraction, is caused by the double-layer repulsion, which is long-range because of the low ionic strength. The long-range repulsion decreases the effective polydispersity of the system. In general, the crystal structure of the lattice is determined by parameters such as particle number density, surface charge, ionic strength, and particle diameter. On the basis of the symmetry of the first layer (we could not image the second layer) and the low ionic strength, we expect the crystal to be fcc.[60]

When we tried to grow colloidal crystals in a capillary, we obtained only amorphous, glasslike, arrangements of spheres (Figure 7c,d). This was caused both by the fact that it is harder to keep the ionic strength sufficiently low in a capillary and by the increased weight of silver dispersion compressing the system. The particles described

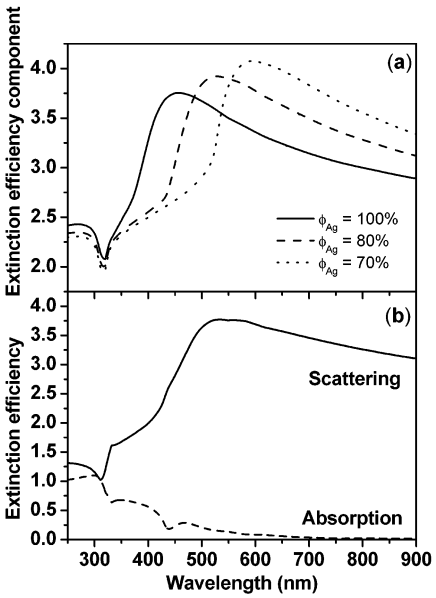

Figure 6. Theoretical extinction efficiency spectra of silver particles ($R = 285$ nm, $\delta = 15\%$) dispersed in water. (a) Extinction efficiency assuming 70% (solid line), 80% (dashed line), and 100% (dotted line) bulk silver in a single particle. The effective dielectric constant was calculated using the Bruggeman effective medium model. (b) Theoretical scattering (solid line) and absorption (dashed line) efficiency components of the total extinction for $\phi_{\mathrm{Ag}} = 80\%$.

(55) Jonson, P. B.; Christy, R. W. *Phys. Rev. Lett.* **1972**, *6*, 4370.
(56) Bohren, C. F.; Huffman, D. R. *Absorption and scattering of light by small particles*; Wiley: New York, 1983.
(57) Kreibig, U.; Vollmer, M. *Optical properties of metal clusters*; Springer: Berlin, 1995.
(58) Kofke, D. A.; Bolhuis, P. G. *Phys. Rev. E* **1999**, *59*, 618.
(59) Auer, S.; Frenkel, D. *Nature* **2001**, *413*, 711.
(60) Hoogenboom, J. P.; Yethiraj, A.; van Langen, A. K.; Romijn, J.; van Blaaderen, A. *Phys. Rev. Lett.* **2002**, *89*, 256104.

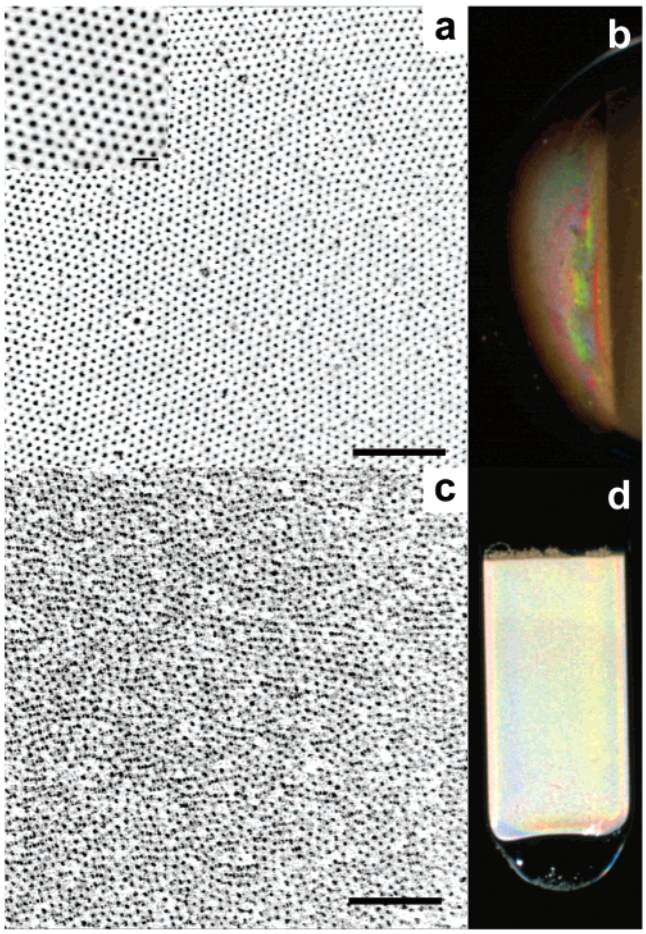

Figure 7. Confocal images (a,c) in reflection mode ($\lambda = 632$ nm) and optical photographs (b,d), under illumination with white light, of samples of Ag particles dispersed in water. (a) Charge-stabilized crystal of silver spheres in water ($R = 257$ nm, $\delta = 17\%$). The spacing between the particles is $\sim 1\,\mu$m. The scale bar is 10 μm. The inset shows a single crystal domain. The inset scale bar is 2 μm. (b) Reflection colors from a charge-stabilized crystal formed at the round bottom of a glass flask (the picture is rotated 90° clockwise). (c) Amorphous glasslike sample of Ag particles ($R = 418$ nm, $\delta = 13\%$). The scale bar is 10 μm. (d) Diffuse reflection colors from a colloidal glass formed in a thin glass capillary.

in the present paper can therefore not be crystallized at the volume fractions that are necessary (>50%) to open up a CPBG.[10] In the glassy sample, only short-range order remains. In both cases, however, these structures display reflection colors when the samples are illuminated with white light. In the case of a crystal (Figure 7b), these colors are much brighter in contrast to the colloidal glass where the colors are more diffuse (Figure 7d). The optical characterization of these glasses and crystals is described elsewhere.[61]

Conclusions

In conclusion, we developed a simple method to synthesize large silver colloidal particles with radii larger than 100 nm via controlled aggregation of silver nanocrystals. The final particle radius can be controlled by the pH of the reaction mixture and the concentration of the reactants. The resulting particles are spherical aggregates with a low polydispersity (<20%) and surface roughness on the order of 10 nm, as determined by electron microscopy. The particles were coated with a protective silica layer without using a silane coupling agent. Good correspondence with scattering theory was found when an effective dielectric constant modeled by the Bruggeman effective medium model was used. The porosity of the particles was in the range of 15−25%. At low volume fraction, the silver particles could be crystallized in charged stabilized colloidal crystals. At higher volume fractions, only glassy structures were obtained.

Acknowledgment. We thank Alexander Moroz (Utrecht University) for inspiring this research, Christina Graf (Utrecht University) for helpful discussions, and Paul van Ekeren (Utrecht University) for performing the TGA analysis. This work is part of the research program of the Stichting voor Onderzoek der Materie, which is financially supported by the Nederlandse Organisatie voor Wetenschappelijk Onderzoek.

LA026610P

(61) Velikov, K. P.; Vos, W. L.; Moroz, A.; van Blaaderen, A. In preparation.